Modulation of leukocyte homeostasis in atherosclerosis

Medina Rodriguez, I.A.

Hematopoietic NAMPT Over–Expression Attenuates Atherosclerosis

Beatriz Bermudez, Indira Medina, Tuva B. Dahl, Mathijs Groeneweg, Jeroen J.T. Otten, Veronica Herias, Jeffrey Pol, Mat Rousch, Sverre Holm, Lourdes M. Varela, Almudena Ortega, Rocio Abia, Laszlo Nagy, Pal Aukrust, Francisco J.G. Muriana, Bente Halvorsen, Erik A.L. Biessen.
Submitted

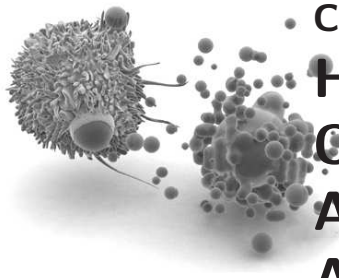

Chapter 3
Hematopoietic NAMPT Over-Expression Attenuates Atherosclerosis

"...society will need to shed some of its obsession for causality in exchange for simple correlations: not knowing why but only what". V. Maker & K. Cukier, Big Data

3.1 Abstract

Background: Besides its presumed cytokine function, NAMPT is a rate limiting enzyme in the NAD^+/NADH biosynthesis salvage pathway. NAMPT confers resistance to apoptosis and oxidative stress, and has been implicated in inflammatory processes and upregulation genes involved in macrophage differentiation and cholesterol. Herein, the role of NAMPT in atherosclerosis was addressed.

Methods and Results: NAMPT was progressively over expressed in human carotid artery atherosclerotic lesions and upregulated in peripheral blood mononuclear cells from stroke patients. $LDLr^{-/-}$ mice with hematopoietic intracellular NAMPT over expression ($iNAMPT^{hi}$) showed attenuated plaque burden with features of lesion stabilization such as reduced apoptotic cell and macrophage contents and lessened necrotic core formation. No significant differences in smooth muscle cells and collagen contents where observed in $iNAMPT^{hi}$ $LDLr^{-/-}$ chimeras. Similarly, no differences were observed in plasma cholesterol, triglyceride and inflammatory cytokine levels, including NAMPT. However, over expressing iNAMPT chimeric mice had reduced circulating monocytes, which were $Ly6c^{lo}$ skewed. In addition, induction of NAMPT over expression upregulated SIRT1, ABCA1 and ABCG1 leading to reduced foam cell formation, and alternative macrophage polarization. Furthermore, iNAMPT inhibited monocyte stromal egress and extravasation in a PPARγ dependent manner by quenching CCR2 expression and migratory capacity. The cross talk between iNAMPT and PPARγ was corroborated in human carotid atherosclerosis, showing a correlation between iNAMPT and PPARγ in atherosclerotic but not healthy arteries.

Conclusions: These findings unveil a critical role for the iNAMPT–PPARγ axis in atherosclerosis, which regulates monocyte egress and migration and macrophage survival and differentiation in atherosclerosis.

3.2 Introduction

Nicotinamide Phosphoribosyl Transferase (NAMPT) or Visfatin was originally reported in 1994 as a pre–Bcell colony enhancing factor (PBEF), secreted protein by activated lymphocytes in bone marrow stroma, suggesting a cytokine like function [152, 153].

In mammals, NAMPT catalyzes a rate limiting first step in the salvage pathway of nicotinamide adenine dinucleotide (NAD^+) synthesis [154], a key factor in cellular energy metabolism and redox homeostasis [155], and cytoprotection. In addition, NAD^+ acts as cofactor for the silent mating type information regulation 2 homolog 1 (SIRT1) [156], which is closely involved in the epigenetic regulation of Peroxisome Proliferator Activated Receptor–γ (PPARγ), Nuclear Factor–κB (NFκB), p53, FOXO transcription factors, and endothelial nitric oxide synthase [157–159]. Moreover, a recent study has implicated NAMPT in the control of granulocyte colony stimulating factor (G–CSF) induced granulopoiesis in healthy subjects and in individuals with severe congenital neutropenia, largely by promoting SIRT1 dependent G–CSF activity [160]. These new studies have considerably widened its potential biological activities beyond that of being a growth factor for B cells.

NAMPT not only acts intra- but also extra–cellularly. Although the physiological role of the extracellular NAMPT (eNAMPT) is still controversial, some studies have imputed eNAMPT pro–inflammatory activity in monocytes, neutrophils, and macrophages. Accordingly, various inflammatory stimuli such as IL–1β, IL–6, TNFα, LPS, IL–8, and oxidized LDL (oxLDL) were seen to induce eNAMPT in $CD14^+$ monocytes [161]. Of note, increased plasma levels of eNAMPT following mechanically induced plaque rupture (i.e., percutaneous coronary intervention) are observed in patients with coronary artery disease. Similarly, enhanced expression of NAMPT is present in unstable atherosclerotic carotid lesions, primarily located to foam cell macrophages [162]; which suggest that both extracellular and iNAMPT may be involved in certain inflammatory disorders such as atherosclerosis.

The latter finding, combined with the reported role of NAMPT in regulating redox homeostasis, apoptosis, and immune responses, all key processes in the lipid driven chronic inflammatory disorder of atherosclerosis, pleads for a contributory role of NAMPT in the progression of this disease. However, despite the wealth of circumstantial evidence, the role of NAMPT in atherosclerotic plaque development has not yet been investigated.

This study demonstrates upregulation of intracellular NAMPT in peripheral blood mononuclear cells (PBMC) of patients with ischemic stroke as well as in human atherosclerotic arteries. Moreover, supraphysiological human iNAMPT expression in hematopoietic cells of LDL receptor deficient ($LDLr^{-/-}$) mice was seen to lead to increased myeloid cell survival and impaired stromal egress with concomitant reduction of circulatory monocytes, which translated in delayed atherosclerotic plaque development. The observed phenotypic effects of iNAMPT on monocytes were demonstrated to proceed in a PPARγ dependent manner. Thus, this study identify the iNAMPT PPARγ pathway as a promising target for the treatment of inflammatory diseases, particularly atherosclerosis.

3.3 Materials and Methods:

PBMC Isolation: PBMC from patients with symptomatic carotid atherosclerosis and healthy controls, recruited from the same area of Norway, were isolated from heparinized blood by Isopaque–Ficoll (Lymphoprep; Nycomed, Oslo, Norway) gradient centrifugation.

Tissue Sampling from Atherosclerotic and non Atherosclerotic Vessels: Atherosclerotic carotid arteries were obtained from patients undergoing carotid endarterectomy (Maasland Hospital, Sittard, The Netherlands and Oslo University Hospital Rikshospitalet, Oslo, Norway) or at autopsy (Department of Pathology, Academic Hospital Maastricht, Maastricht, The Netherlands) as previously described [162,163]. Lesions obtained in The Netherlands, were scored according to the criteria of Virmani and coworkers [95]. Intimal thickening was classified as early, thick fibrous cap atheroma as advanced, and thin cap fibroatheroma with features of cap break, mural thrombi, plaque dissection and/or intraplaque hemorrhage were regarded as ruptured lesions. Non atherosclerotic vessels were obtained from common iliac artery of organ donors (Oslo University Hospital Rikshospitalet, Oslo, Norway) and the samples were handled and stored following the same protocol as that used for the atherosclerotic vessels.

Animals: Female and male LDLr$^{-/-}$ mice, on C57/Bl6 background, were obtained from the local animal breeding facility at University of Maastricht. Mice were fed a regular chow diet (SDS, Essex, UK). Female LysM–Cre–PPAR$\gamma^{flox/flox}$ bones were kindly provided by Prof. Nagy (University of Debrecen, Hungary). Drinking water and food were provided *ad–libitum*. Experiments were performed at the animal facility of the University of Maastricht. Male LDLr$^{-/-}$ mice were used as donors for bone marrow transplantations and in vitro assays. All study protocols involving animal experiments were approved by the Animal Care and Use Committee of the University of Maastricht and were performed according to official rules formulated in the Dutch law on care and use of experimental animals.

Lentivirus Production and Transfection: Plasmids encoding NAMPT, pRRL–PGK–hNAMPT and pRRL–PGK–Empty Lentivirus vectors were used. Human NAMPT (GenBank accession number NM005746.2) complementary DNA (cDNA) was polymerase chain reaction (PCR) amplified, sequenced, and subcloned into pRRL–PGK Lentivirus vector. Plasmids for lentiviral packaging, pMDLg/pRRe, pRSV–REV, and pMD2G were obtained from Addgene (Cambridge, USA). Recombinant lentivirus were produced by transfecting lentivector and packaging vectors into 293T cells (Invitrogen, Paisley, UK).

Bone Marrow Transplantation: Female LDLr$^{-/-}$ (n = 50) mice were lethally irradiated with a single dose (9 Gy; 0.5 Gy/min; MU 15F/225 kV; Philips) to induce bone marrow aplasia one day before transplantation. Mice were maintained in filter–top cages and given water containing 60,000 U/l polymyxin B sulfate (Invitrogen) and 100 mg/l neomycin (Invitrogen) starting 1 week before bone marrow transplantation. Bone marrow was isolated from male LDLr$^{-/-}$ donors by flushing their femurs

and tibiae. Bone marrow cells were plated (10^7/well) in DMEM supplemented with 10% FCS, L–glutamine, penicillin/streptomycin, and 10μg/ml DEAE–dextran, and infected either with empty or NAMPT containing lentiviral particles (multiplicity of infection, MOI=15:1) for 24 h [164]. The next day, irradiated recipients received an intravenous tail vein injection with a total of 5x10^6 infected bone marrow cells per mouse. Drinking water supplemented with antibiotics as indicated above was provided ad libitum for 6 weeks post–transplantation. Thereafter, control and iNAMPT chimeras (mice transplanted with bone marrow transfected with either empty or hematopoietic iNAMPT containing vector (iNAMPT^{hi})) were fed WTD, containing 0.25% cholesterol and 15% cacao butter (SDS, Essex, UK) for 6 and 12 weeks and subsequently sacrificed.

Histological Analysis: Aortic root sections were collected and then were formalin fixed and paraffin embedded. Subsequently, 4μm thick sections were cut and stained with haematoxylin and eosin (HE). Lesion size and necrotic core area were determined based on this staining in three to five sections per animal. Corresponding sections on separate slides were stained with an antibodies against MAC3 (Becton Dickinson, NJ, USA), ASMA (Sigma–Aldrich), and Caspase–3 (Cell Signaling Technology). Sirius Red staining was performed to detect collagen. Histological analyses were performed, in a blinded manner, by an independent operator using Quantimet with Qwin3 quantification software (Leica).

Flow Cytometry: Upon sacrifice, blood, spleen, and bones from the mice were collected. Single cell suspensions were made from spleen. Erythrocytes in blood and spleen were removed by incubation with a hypotonic buffer (8.4 g/l NH_4Cl and 0.84 g/l $NaHCO_3$, pH 7). Non–specific Fc–receptor binding of antibodies was blocked by addition of an anti–CD16/CD32 antibody (eBioscience, San Diego, USA). To determine lymphocyte subsets, cells were labeled with the following antibodies: CD3e–FITC, CD8a-eFluor450, B220-PE-Cy7, CD25-APC, FoxP3-PE (all from eBioscience), and CD4-PerCP (BD). To detect monocytes and granulocytes, the cells were labeled with antibodies against CD11b-PerpCy5.5 (BD), Ly6G-PE (eBioscience), CXCR4-APC (BD), CD62L-PE-Cy7 (eBioscience), and Ly6C-FITC (Miltenyi Biotec, BG, Germany). After labeling, the samples were analyzed on a FACS Canto II flow cytometer (BD). Samples and buffers were kept on ice throughout the experiments.

Colony Forming Units Assay: Bone marrow cells were isolated from one tibia and one femur per mouse, as previously described [83]. Cells were counted twice manually using a count chamber and the concentration was calculated for each sample. Per well, 10.000 bone marrow cells were added to 2 ml methyl cellulose medium with recombinant cytokines (MethoCult Medium, StemCell Technologies, Grenoble, France). After incubation for 7 days, at 37^{o}C and 5% CO2, the total number of colonies was quantified by an independent operator. Besides total number of colonies, GM–CFU, G–CFU, and M–CFU colonies were specified based on morphology.

Macrophage Culture: Bone marrow cells were isolated from control and iNAMPT^{hi} chimeras (n = 5 mice/group). From each chimera, cells were pooled and cultured in

RPMI (Invitrogen) containing 10% heatinactivated fetal calf serum, 100 U/ml penicillin, 100 g/ml streptomycin, 2 mM L–glutamine, 10 mM Hepes, and supplemented with 15% L929–conditioned medium to generate bone marrow derived macrophages (BMDMs) [165]. Medium was replaced every three days and differentiated BMDMs were used for in vitro assays seven to eight days after isolation.

M1/M2 Polarization: BMDM polarization was obtained by removing the culture medium and culturing cells for an additional 24 h in RPMI (Invitrogen) supplemented with 10% FCS and 100ng/ml LPS plus 20ng/ml IFNγ (for M1 polarization) or 20 ng/ml IL–4 (for M2 polarization). Quantitative gene expression of cytokines, M1, and M2 macrophage markers were analyzed as previously described [166, 167]. Total RNA was isolated from BMDMs using Tri–Reagent (Sigma), according to the manufacturer's protocol. RNA concentration was measured in a NanoDrop spectrophotometer (Witec AG, Switzerland). One microgram total RNA was used to obtain cDNA (iScript, BioRad), according to the manufacturers protocol. The qPCR Mastermix Plus kit for SYBR green (Eurogentec) was used on 10ng cDNA. Analysis was performed on an iCycler IQ5 (BioRad). The reference genes 18s and β–actin were used to correct for RNA concentration differences between samples. Primers were designed based on PRIMER3.0. Primer sequences can be found in Table 3.1.

Gene	Forward Primer	Reverse Primer
18s	5'CGCGGTTCTATTTTGTTGGT3'	5'AGTCGGCATCGTTTATGGTC3'
CCR2	5'AGAGAGCTGCAGCAAAAAGG3'	5'GGAAAGAGGCAGTTGCAAAG3'
CCL2	5'AGGTCCCTGTCATGCTTCTG3'	5'TCTGGACCCATTCCTTCTTG3'
TNFα	5'AGCCCCCAGTCTGTATCCTT3'	5'CTCCCTTTGCAGAACTCAGG3'
IL–1β	5'GCCCATCCTCTGTGACTCAT3'	5'AGGCCACAGGTATTTTGTCG3'
PPARγ	5'TTTTCAAGGGTGCCAGTTTC3'	5'AATCCTTGGCCCTCTGAGAT3'
ABCA1	5'AACAGTTTGTGGCCCTTTTG3'	5'AGTTCCAGGCTGGGGTACTT3'
ABCG1	5'GTACCATGACATCGCTGGTG3'	5'AGCCGTAGATGGACAGGATG3'
IL–10	5'CCAAGCCTTATCGGAAATGA3'	5'TTTTCACAGGGGAGAAATCG3'
MR1	5'ATGCCAAGTGGGAAAATCTG3'	5'TGTAGCAGTGGCCTGCATAG3'
ARG1	5'GTGAAGAACCCACGGTCTGT3'	5'CTGGTTGTCAGGGGAGTGTT3'
iNOS	5'CACCTTGGAGTTCACCCAGT3'	5'ACCACTCGTACTTGGGATGC3'
IL–6	5'AGTTGCCTTCTTGGGACTGA3'	5'TCCACGATTTCCCAGAGAAC3'
β-actin	5'AGCCATGTACGTAGCCATCC3'	5'CTCTCAGCTGTGGTGGTGAA3'

Table 3.1. *Primers Used for M1/M2 macrophage polarization in iNAMPT over expressing BMDM.*

Migration Assay: In wound healing assays, BMDM were cultured to confluence on tissue culture plates. An in vitro wound generated by scratching with the blunt end of a 200μl plastic pipette tip, was created and the edge of the wound was marked. Cell migration was observed by phase contrast microscopy. Complete medium, including 500 nM of NAMPT inhibitor (FK866, Cayman Chemical), was added to the wells and cells were allowed to migrate for up to 24 h. The chemotactic peptide

N–formyl–methionyl–leucyl–phenylalanine (fMLP, Sigma) was used (1 nM) as a positive control. The number of cells that had completely migrated to the wound side was scored.

LDL Isolation and Modification; Fresh blood (obtained from healthy volunteers) was incubated for 30 min at 37^{o}C followed by 30 min at 4^{o}C in 50 ml Falcon tubes. Subsequently, the blood was centrifuged at 4,000 rpm for 10 min to isolate the serum. The serum was brought to a density of 1.21 g/ml with KBr and put in a NaCl gradient in 25x89 mm Ultratubes and centrifuged at 25.000 rpm in a Beckman SW28.1 rotor for 18 h at 4^{o}C. The LDL fraction was isolated and treated with 25μM $CuSO_4$ at 37^{o}C overnight to be oxidized. Oxidation was stopped by adding 50μM EDTA. This protocol was adapted from [87]. All lipoproteins were dialyzed against PBS containing 10μM EDTA, and stored at 4^{o}C under N_2 for a maximum of 2 weeks. Concentration was measured using the BioRad BCA protein assay kit (Pierce, USA). Samples containing serum, LDL or oxLDL were tested for endotoxins using a Limulus Amebocyte Lysate (LAL) assay (HyCult Biotech, The Netherlands) according to the manufacturer's protocol. Endotoxin concentration of all samples was below 5 pg/ml.

Apoptosis Assay: BMDM were cultured as described above and plated in 48-wells plates (Corning, Lowell, MA, USA). Cells were incubated for 18 h in plain medium or medium supplemented with camptothecin (CPT, 500μM) or oxLDL (50μg/ml) to induce apoptosis. Cells were labeled with Annexin-V Alexa-488 (Invitrogen) and stained with propidium iodide to detect apoptosis and necrosis, respectively. Pictures were made using a Leica microscope (Leica) with Qwin software. Subsequently overlays were analyzed with ImageJ Software to quantify the number of apoptotic and necrotic cells per field.

Lipid Uptake Assay: LDL was labeled by adding 150μl of 3mg/ml 1,1'–dioctadecyl–3,3,3',3'–tetra–methyl–indocarbocyanine–perchlorate (DiI) in DMSO to 3 ml LDL (0.5 mg/ml) overnight. After labeling, the unbound DiI was removed using a PD10 column (Amersham Biosciences). BMDM were incubated with 50μg/ml labeled oxLDL for 3 h, with and without 500 nM of NAMPT inhibitor (FK866). As a control, BMDM were also incubated with DMSO. Cells were lifted from the culture dish and washed 3 times with PBS. Finally, the cells were resuspended in 200μl PBS and analyzed using flow cytometry in a FACS Canto II (BD Biosciences).

Lipid Extraction and TLC: BMDM were scraped from plastic 6-well plates, suspended in 200μl PBS and frozen at 20^{o}C. The cells were defrosted and repeatedly passed through a syringe to fully lyse them. Cell lysates were further treated for lipid analysis as described before [88].

Ethics: The human parts of the study were approved by the local ethical committee and conducted according to the ethical guidelines outlined in the Declaration of Helsinki for use of human tissue and subjects. Informed written consent was obtained from all subjects. All animal experiments were carried out in accordance with institutional guidelines, and conform to the Guide for the Care and Use of Laboratory

Animals published by the US National Institutes of Health (NIH Publication No. 85-23, revised).

Cholesterol Measurements: Blood samples of mice were collected upon sacrifice and plasma (100μl) was stored at 80^{o}C for further use. Plasma cholesterol levels were measured using a colorimetric assay (CHOD–PAP, Roche, Mannheim, Germany).

NAD+ and Cytokine Determinations: Intracellular NAD+ concentrations were determined by an enzymatic cycling assay. Cells were lysed in NAD^+ extraction buffer containing 100 mM Na_2CO_3 and 20 mM $NaHCO_3$. Samples (20μl) were mixed with a cycling buffer (160μl) containing 125 mM Tris HCl pH 8.8, 1.25 mM phenazine ethosulfate, 0.625 mM thiazolyl blue tetrazolium bromide (MTT), 0.25 mg/ml alcohol dehydrogenase, and 1.25% BSA (all from Sigma). The cycling reaction was initiated by adding 20μl of ethanol 6 M. After sample incubation for 10 min at 37^{o}C, the optical density at 570 nm was measured using an ELISA plate reader. Serial dilutions of NAD^+ were used as a standard. NAD^+ concentrations were normalized to protein concentrations. Cytokines were determined in plasma by using the Bio–Plex Pro mouse cytokine 23–plex immunoassay (BioRad) according to the manufactures protocol.

Statistical Analysis: Data are expressed as mean±SEM. A two tailed Students t–test was used to compare individual groups. Non–parametric data were analyzed using Mann–Whitney U test. Correlations were analyzed by Spearman rank test, while distribution variances were analyzed by F–test. All analyses were performed using GraphPad Prism 5 software (GraphPad Software Inc, La Jolla, CA, USA) and MATLAB. P–values below 0.05 were considered to be statistically significant.

3.4 Results

NAMPT is Upregulated in Circulating Leukocytes and Atherosclerotic Lesions of Patients with Carotid Atherosclerosis Increased expression of NAMPT in carotid lesions of patients with symptomatic disease (i.e., stroke or transient ischemic attack) has been previously reported [162]. In the present study, these findings were extended by demonstrating that these patients also show a profound upregulation of NAMPT gene expression in PBMC (Fig. 3.1A). In addition, NAMPT was also upregulated in human atherosclerotic samples obtained during carotid endarterectomy. Furthermore, the relative gene expression levels of NAMPT increased progressively from early stable lesions to advanced and ruptured plaques (Fig. 3.1B).

Hematopoietic Human iNAMPT Over Expression Attenuates and Stabilizes Atherosclerotic Lesions in LDLr$^{-/-}$ Atherosclerotic Mice The functional implications of dysregulated NAMPT expression on plaque development were next addressed, considering that it is a characteristic trait underlying the pathophysiology of cardiovascular diseases. To approach this, chimeric LDLr$^{-/-}$ mice over expressing human iNAMPT (iNAMPT^{hi}) in the hematopoietic compartment were generated, by reconstitution of irradiated recipient mice with PGK–NAMPT lentivirus infected bone marrow [126].

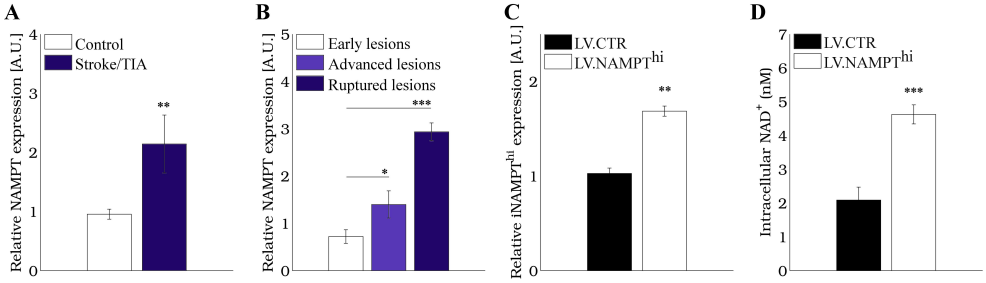

Figure. 3.1. *Expression of NAMPT in PBMCs and atherosclerotic plaques from patients with Cardiovascular Disease; and bone marrow cells from LDLr$^{-/-}$ mice recipients of bone marrow cells transfected with lentivirus encoding iNAMPT. A. NAMPT is over expressed in PBMCs obtained from patients with ischemic stroke and transient ischemic attack (TIA) compared to healthy subjects. B. NAMPT mRNA expression is higher in human carotids with advanced and ruptured atherosclerotic plaques, compared to early lesions. C-D. NAMPT mRNA expression and intracellular NAD$^+$ were determined in bone marrow cells from irradiated LDLr$^{-/-}$ recipients reconstituted with LV.CTR (Empty vector) (black bars) or LV.NAMPT^{hi} (open bars) infected bone marrow cells from LDLr$^{-/-}$ donors (n=12). Data as mean ±SEM. $*P \leq 0.05$, $**P \leq 0.01$, $***P \leq 0.001$.*

Chimeric mice with the empty vector control PGK were also generated, to serve as control for the experiments. After recovery from BMT for 6 weeks, mice were fed a WTD for 6 and 12 weeks for analysis of early and advanced lesion development, respectively. Hematopoietic iNAMPT over expression did not influence body weight (Appendix B. Fig. B1A) nor total plasma cholesterol or triglyceride levels (Appendix B. Fig. B1B-C) in WTD–fed chimeric mice. At sacrifice, bone marrow cells of the iNAMPT^{hi} chimera displayed supraphysiological expression of iNAMPT (+65%, $P \prec 0.01$; Fig. 3.1C), an effect that was accompanied by almost 2-fold increased intracellular NAD$^+$ levels (Fig. 3.1D).

Early lesion development (6 weeks of WTD) in the aortic roots did not differ between the iNAMPT^{hi} and control chimeras (Fig. 3.2A). In contrast, plaque area was significantly diminished in the iNAMPT^{hi} chimera at 12 weeks of WTD feeding (Fig. 3.2B). At this point, necrotic core size (Fig. 3.2B) and plaque macrophage contents (Fig. 3.2C) were more than 50% decreased in the iNAMPT^{hi} chimera. The proportion of intimal apoptosis as assessed by activated Caspase-3 was also reduced (Fig. 3.2D). Of note, neutrophil (Appendix B. Fig. B2A), T–lymphocytes (Appendix B. Fig. B2B), and VSMC (Appendix B. Fig. B2C) numbers, as well as collagen contents (Appendix B. Fig. B2D) were similar in the plaque of the iNAMPT^{hi} and control chimeras.

Hematopoietic Human iNAMPT Over Expression Acts Cytoprotective and Increases Medullar Myelopoiesis Assessment of the susceptibility to apoptosis induction indicated that over expression of iNAMPT acted cytoprotective. In fact, iNAMPT^{hi} chimeras displayed increased resistance to camptothecin (CPT) or oxLDL

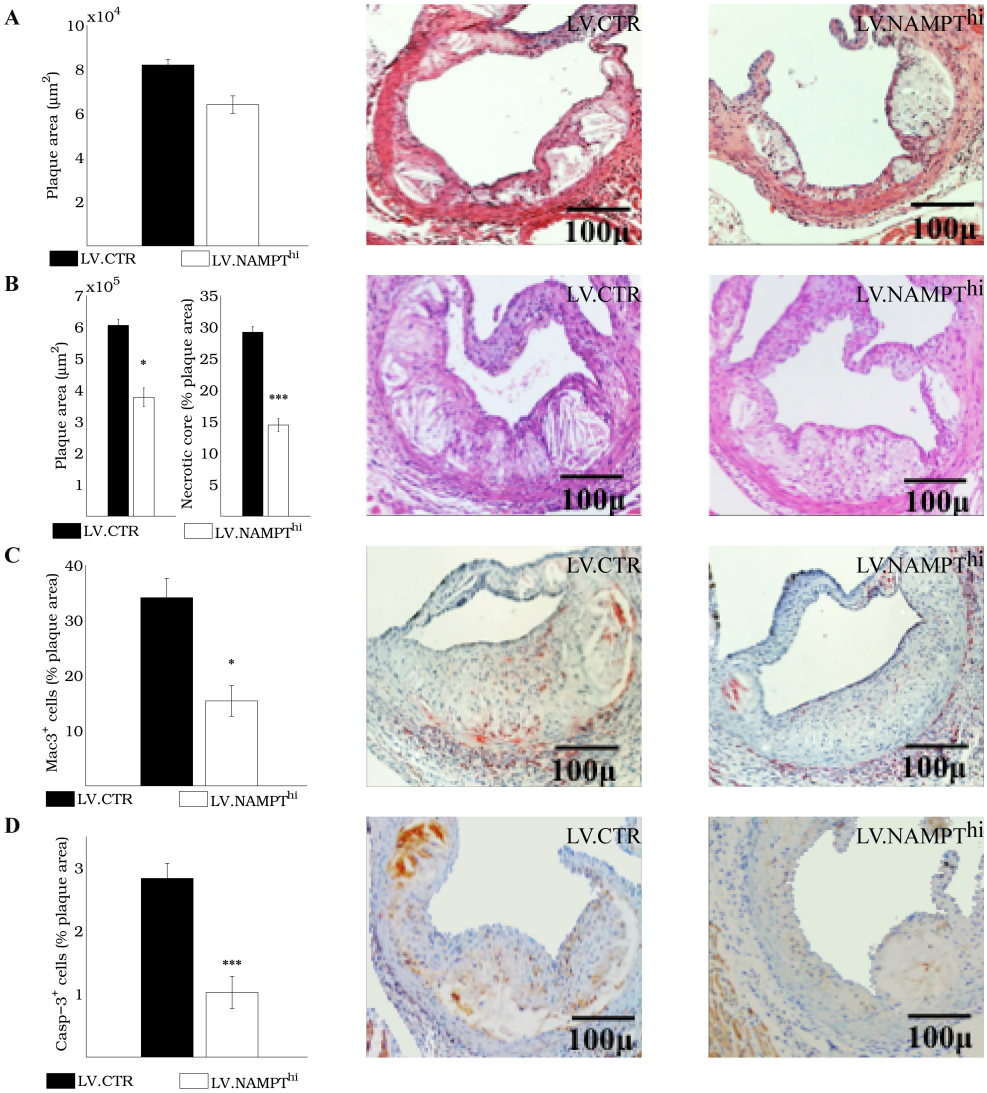

Figure. 3.2. *Hematopoietic iNAMPT over expression attenuates atherosclerotic lesion development in LDLr$^{-/-}$ mice. Bone marrow of irradiated LDLr$^{-/-}$ recipients was reconstituted with LV.CTR (Empty lentivirus vector) or LV.NAMPT^{hi} (NAMPT expressing vector) infected bone marrow cells from LDLr$^{-/-}$ donors. Atherosclerotic lesion size was not altered 6 weeks after introduction of atherogenic diet (A) but was significantly reduced 12 weeks on atherogenic diet (B) when necrotic core (B), macrophage (C) and apoptotic cell (D) contents, relative to lesion area, were reduced (n=12). Middle and right panels in A-D display representative pictures of HE (A-B), Mac-3 (C) and activated Caspase-3 (D) stainings used for quantification of LV.CTR (middle panel) and LV.NAMPT^{hi} (right panel) chimeras. Data as mean $\pm SEM$. $*P \leq 0.05$, $**P \leq 0.01$, $***P \leq 0.001$.*

induced cytotoxicity. (Fig. 3.3A). In addition, analysis of bone marrow cells obtained from iNAMPT^{hi} mice demonstrated increased levels of total colony forming units (CFU), compared to the controls (Fig. 3.3B). This effect could be almost entirely ascribed to an increased frequency of CFU-GM, CFU-G, and CFU-M (Fig. 3.3C), suggesting a myeloproliferative response to hematopoietic iNAMPT over expression.

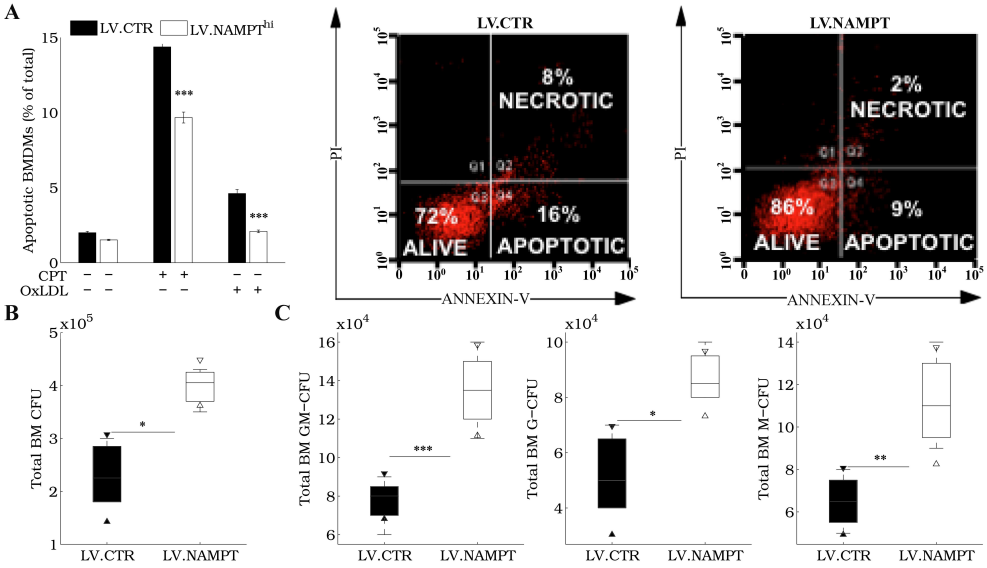

Figure. 3.3. *Hematopoietic iNAMPT over expression modulates the survival of myeloid cells and increases bone marrow myelopoiesis in LDLr$^{-/-}$ Mice. Bone marrow of irradiated LDLr$^{-/-}$ recipients were reconstituted with LV.CTR (Empty vector) or LV.NAMPT^{hi} infected bone marrow cells from LDLr$^{-/-}$ donors. A. Apoptosis quantification by flow cytometry (Annexin V and PI staining) in bone marrow derived macrophages (BMDM) obtained from mice chimeras after 24 h incubation with CPT (1 nM) or oxLDL (50µg protein/ml). Representative pictures of flow cytometry analysis after CPT incubation are shown in the right part of the panel. B-C. Quantification of colony forming units (CFU) in BMC from LDLr$^{-/-}$ recipients reconstituted with LV.CTR or LV.NAMPT^{hi} infected BMC from LDLr$^{-/-}$ donors. Total CFU (B) granulocyte and macrophage (GM), granulocyte (G) and macrophage (M) CFU (C) were increased in NAMPT over expressing chimeras (n=12). Data as mean ±SEM. $*P \leq 0.05$, $**P \leq 0.01$, $***P \leq 0.001$ compared to the control chimera.*

Hematopoietic Human iNAMPT Over Expression Alters Myeloid Stromal Egress

Granulocyte and monocyte numbers in bone marrow and blood of chimeric mice were quantified to assess the systemic effect of iNAMPT induced myeloproliferation. Relative bone CD11b^{+}Ly6G^{+} granulocyte and CD11b^{+}Ly6G^{-} monocyte counts were slightly but significantly augmented in iNAMPT^{hi} chimeras (Fig. 3.4A-B). However, granulocyte levels in the bloodstream were unchanged by hematopoietic iNAMPT over expression (Fig. 3.4C). In addition, circulatory monocyte counts were lower in

the iNAMPT^{hi} chimeras (Fig. 3.4D).

Similar discrepancies in bone marrow and blood homeostasis were observed for activated granulocytes and monocyte subsets. In fact, the relative proportion of CD62L^{lo}CXCR4^{hi} granulocytes within the total granulocyte population was unchanged in the bone marrow (Fig. 3.4E), where higher levels of Ly6c^{lo} monocytes were observed, leading to a lower Ly6C^{hi}/Ly6c^{lo} ratio (Fig. 3.4F). In contrast, circulatory CD62L^{lo}CXCR4^{hi} granulocyte numbers were reduced in NAMPT over expressing chimeras (Fig. 3.4G) and a marked enrichment in anti–inflammatory Ly6c^{lo} monocytes was observed (Fig. 3.4H).

Consistent with an inhibitory role of iNAMPT in bone marrow monocyte mobilization, LDLr$^{-/-}$ mice that were intraperitoneally injected with the NAMPT inhibitor FK866 exhibited a reduction in stromal bone marrow monocyte content (Appendix B. Fig. B3A) and increased numbers of circulating monocytes (Appendix B. Fig. B3B). No changes in the number of circulatory CD3^{-}B220^{+}, CD3^{+}CD4^{+} or CD3^{+} CD8^{+} lymphocytes, and splenic granulocytes or monocytes were detected in the iNAMPT^{hi} versus control chimeras (data not shown).

One of the key regulatory pathways in stromal egress of monocytes has been reported to be the CCR2–CCL2 axis [168]. Compatible with this notion, gene expression analysis of CCR2 and its ligand CCL2 in BMDM from the iNAMPT^{hi} chimera revealed a strong downregulation of the former, whereas CCL2 expression remained unaltered (Fig. 3.5A). Thus, these findings suggest that iNAMPT is a negative regulator of CCR2–dependent monocyte mobilization. In agreement with this notion, non treated and fMLP elicited cell motility was sharply reduced in BMDM of iNAMPT^{hi} versus control chimeras. Conversely, the motile capability of BMDM from FK866 treated mice was augmented (Fig. 3.5B). These findings therefore suggest that iNAMPT over expression might have caused interrupted chemotaxis and reduced monocyte extravasation into atherosclerotic lesions .

iNAMPT Acts Anti–Inflammatory Partly Via PPARγ We next assessed whether PPARγ acted downstream of iNAMPT, as it has been reported to be targeted by SIRT1 [169], an effector enzyme activated by iNAMPT [170], which was recently attributed a variety of anti–inflammatory actions [171]. Genetic loss of function approaches, using BDMDs derived from conditional PPARγ knockout mice LysM–Cre-PPAR$\gamma^{flox/flox}$ [172] were used to determine to what extent the aforementioned iNAMPT effects were mediated via PPARγ. Conditional PPARγ deficient BMDM were then infected with PGK–NAMPT or PGK–Empty lentivirus to generate LysM–Cre-PPAR$\gamma^{flox/flox}$ iNAMPT^{hi} BMDM.

CCR2 and CCL2 were upregulated in BMDM of LysM–Cre–PPAR$\gamma^{flox/flox}$ (Fig. 3.5C). In addition, iNAMPT over expression completely failed to suppress CCR2 expression in PPARγ deficient BMDM. However, over expression of iNAMPT brought the expression of CCL2 back to the level observed in control and iNAMPT^{hi} BMDM (Fig. 3.5C). Moreover, iNAMPT over expression had no effect on PPARγ deficiency associated increase in BMDM migratory capacity (Fig. 3.5D). iNAMPT^{hi} chimeras also featured upregulated expression of PPARγ (+60%, $P \prec 0.01$) and of its regulator SIRT1 (+28%, $P \prec 0.05$) in bone marrow cells, reflective of complex interaction between iNAMPT and PPARγ (Fig. 3.5E).

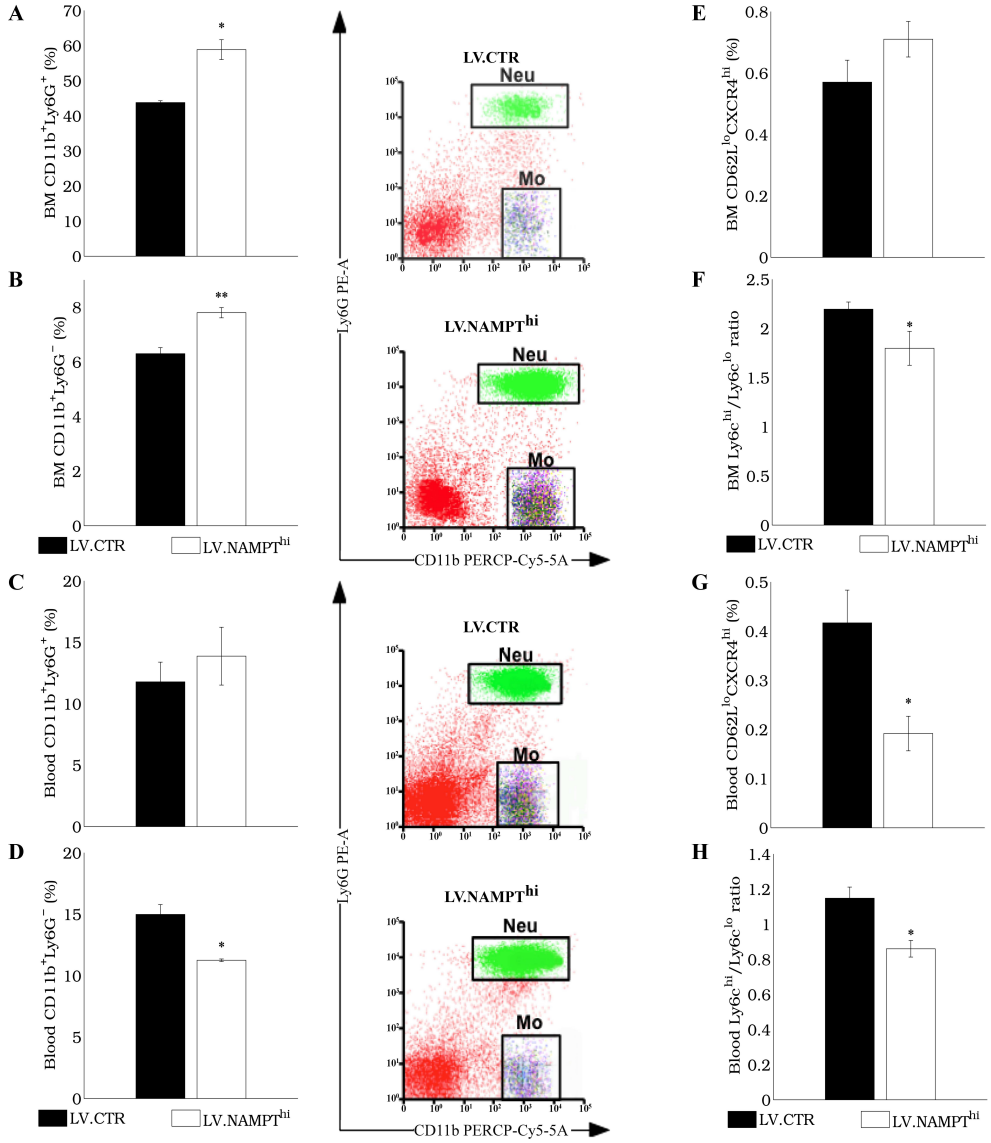

Figure. 3.4. *Hematopoietic iNAMPT over expression perturbs stromal and circulatory leukocyte homeostasis in LDLr$^{-/-}$ mice. Bone marrow of irradiated LDLr$^{-/-}$ recipients was reconstituted with donor LV.CTR (Empty vector) or LV.NAMPT^{hi} infected bone marrow cells. Relative granulocyte (A,C) and monocyte (B,D) contents in bone marrow (A-B) and blood (C-D) of LDLr$^{-/-}$ chimeras, (corresponding graphs of flow cytometry analysis of monocytes and granulocytes are depicted in the right side of the panels). Relative fraction of activated granulocytes (E,G) and Ly6c^{hi}/Ly6c^{lo} ratio (F,H) in bone marrow (E-F) and blood (G-H) of LDLr$^{-/-}$. (Data as mean ±SEM. $*P \leq 0.05$, $**P \leq 0.01$, $***P \leq 0.001$ compared to the control chimera; $n = 12$).*

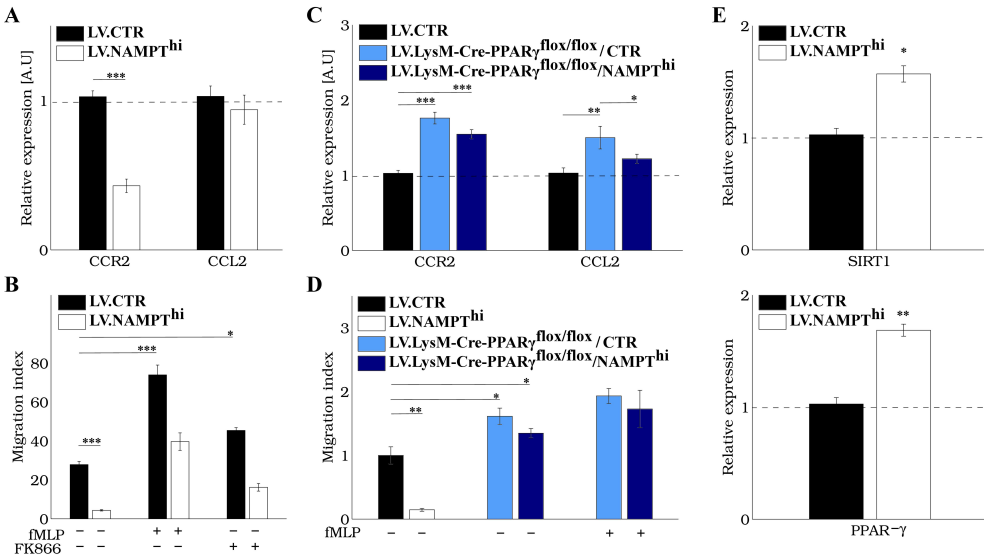

Figure. 3.5. *Hematopoietic iNAMPT over–expression impairs the migratory response of BMDM via PPARγ and upregulates the expression of SIRT1 and PPARγ. Bone marrow of irradiated LDLr$^{-/-}$ recipients was reconstituted with LV.CTR (Empty vector) or LV.NAMPT^{hi} infected bone marrow cells from LDLr$^{-/-}$ donors. A. CCR2 and CCL2 mRNA expression in bone marrow derived macrophages (BMDM) of LDLr$^{-/-}$ chimeric mice recipient of lentivirus transduced bone marrow cells. B. Migration index of BMDM after incubation with fMLP (1 nM) in the absence or presence of FK866 (500 nM). (C) CCR2 and CCL2 mRNA expression in PPARγdeficient BMDM infected with LV.CTR (sky blue bars) or LV–NAMPT^{hi} (dark blue bars) lentivirus. (D) Migration index of PPARγ deficient BMDM infected with LV.CTR (sky blue circles) or LV–NAMPT^{hi} (dark blue circles) lentivirus after incubation with fMLP (1 nM). (E) SIRT1 (top panel) and PPARγ (bottom panel) mRNA expression in BMC. Data as mean ±SEM. $*P \leq 0.05$, $**P \leq 0.01$, $***P \leq 0.001$.*

Hematopoietic Human iNAMPT Over Expression Favors Alternatively Activated Macrophage Polarization Classically activated macrophages (CAM) are deemed to be derived from Ly6c^{hi} monocytes [173,174] and recruited into inflamed tissues partly via CCR2 [175]. CCR2–dependent retention of monocytes in the bone marrow rendered Ly6c^{lo} monocytes, the dominant subset in iNAMPT^{hi} chimeras. We therefore hypothesized that iNAMPT over expression caused macrophage differentiation skewing towards alternatively activated M2 macrophages, known for their wound healing and resolution of inflammation activities [176, 177]. In agreement with this hypothesis, iNAMPT^{hi} BMDM, polarized with IFNγ and LPS (M1) or IL–4 (M2), showed attenuated or increased expression, respectively, of established M1 (TNFα, IL–6, and iNOS) and M2 (IL–10, ARG1, and to a lesser extent MRC1) markers, relative to control BMDM (Fig. 3.6A).

The above identification of PPARγ as an iNAMPT responsible gene, and the

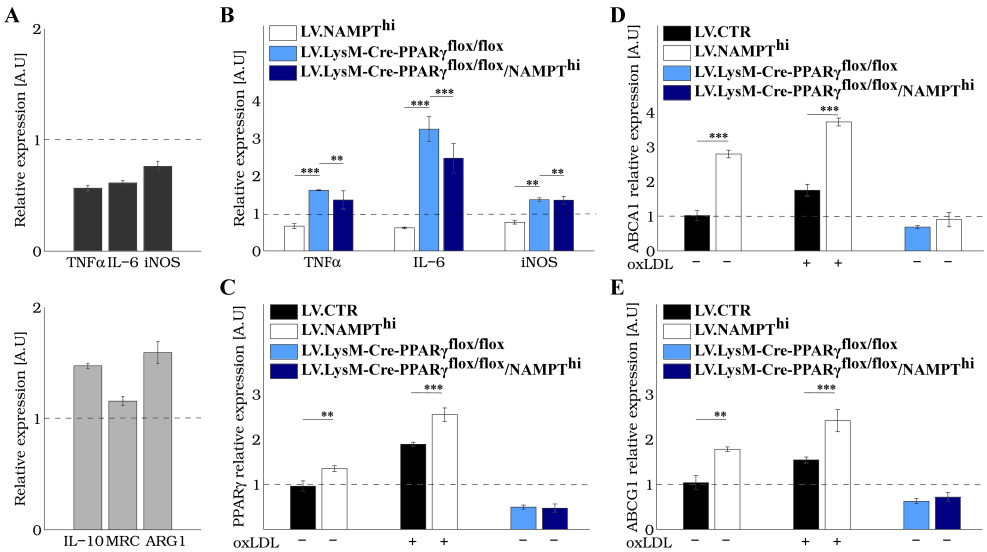

Figure. 3.6. *Hematopoietic iNAMPT over expression favors BMDM alternative anti–inflammatory differentiation. Bone marrow of irradiated LDLr$^{-/-}$ recipients was reconstituted with LV.CTR (Empty vector) (black bars) or LV.NAMPT^{hi} (black bars) infected bone marrow cells from LDLr$^{-/-}$ donors. Bone marrow derived macrophages (BMDM) obtained from chimeric mice was used for further analysis. A. TNFα, IL–6, and iNOS were downregulated in M1 polarized LV.NAMPT^{hi} BMDM (gray bars, top panel). IL–10, MRC, and ARG1 mRNA were in contrast upregulated in M2 polarized LV.NAMPT^{hi} BMDM (light gray bars, bottom panel). B. TNFα, IL–6, and iNOS mRNA expression is conversely upregulated in PPARγ deficient BMDM infected with LV.CTR (sky blue bars). Infection of those cells with LV.NAMPT^{hi} (dark blue bars) lentivirus, dampens this effect. C-E. PPARγ (C), ABCA1 (D), and ABCG1 (E) mRNA expression is upregulated in LV.NAMPT^{hi} BMDM after 24 h incubation with oxLDL (50μg protein/ml). PPARγ deficiency block this upregulation. Data as mean ±SEM. $*P \leq 0.05$, $**P \leq 0.01$, $***P \leq 0.001$, n =4.*

recent finding that this nuclear receptor is a key positive regulator of alternative macrophage polarization [178], suggested the involvement of PPARγ on iNAMPT associated M2 skewed macrophage polarization. As expected, macrophage deficiency in PPARγ (LysM–Cre–PPARγ$^{flox/flox}$) translated in a profound increase in expression of M1 markers; however, unlike control BMDM, iNAMPT over expression did not alter M1 marker gene expression patterns in LysM–Cre–PPARγ$^{flox/flox}$ BMDM (Fig. 3.6B). From these results, PPARγ was demonstrated to be a downstream effector of iNAMPTmediated macrophage reprogramming towards M2–type cells. It is worth noting that hematopoietic iNAMPT over expression did not confer systemic anti–inflammatory effects, as judged by the unaltered plasma cytokine patterns observed in iNAMPT^{hi} compared to control chimeras (Appendix B. Fig. B4A-B).

Hematopoietic Human iNAMPT Over Expression Promotes PPARγ–Responsive Gene Transcription with Functional Consequences in Macrophages The tight interplay between iNAMPT and PPARγ, a master regulator of lipid handling in macrophages [179, 180] and the iNAMPT associated induction of intracellular levels of NAD^+, which may impact lipid metabolism as well [181,182], hinted towards an effect of iNAMPT over expression on macrophage lipid handling. In line with the aforementioned iNAMPT–induced upregulation of PPARγ in BMC, iNAMPT^{hi} BMDM had roughly 30% higher PPARγ mRNA expression in comparison to control BMDM (Fig. 3.6C). LysM–Cre–PPARγ$^{flox/flox}$ BMDM showed intrinsically reduced PPARγ mRNA expression, which was not affected by iNAMPT over expression (Fig. 3.6C). Of note, iNAMPT augmented oxLDL induced PPARγ upregulation in BMDM (Fig. 3.6C).

ABCA1/ABCG1 gene expression patterns essentially mirrored that of PPARγ, with strong iNAMPT over expression associated upregulation in control but not LysM–Cre–PPARγ$^{flox/flox}$ BMDM (Fig. 3.6D-E). Consistent with this, BMDM of iNAMPT^{hi} chimeras accumulated less cholesterol ester than BMDM of control chimeras in either the absence or presence of oxLDL (Fig. 3.7A); however, free cholesterol remained at similar levels in control and iNAMPT^{hi} BMDM after oxLDL administration (Fig. 3.7B). The uptake of DiI–oxLDL was enhanced in BMDM over expressing iNAMPT, an effect that was profoundly diminished in the presence of the NAMPT inhibitor FK866 (Fig. 3.7C), similarly to the lack of effect in LysM–Cre–PPARγ$^{flox/flox}$ BMDM. These findings demonstrate for the first time, that the iNAMPT–PPARγ axis is strongly involved in the modulation of the macrophage lipid homeostasis.

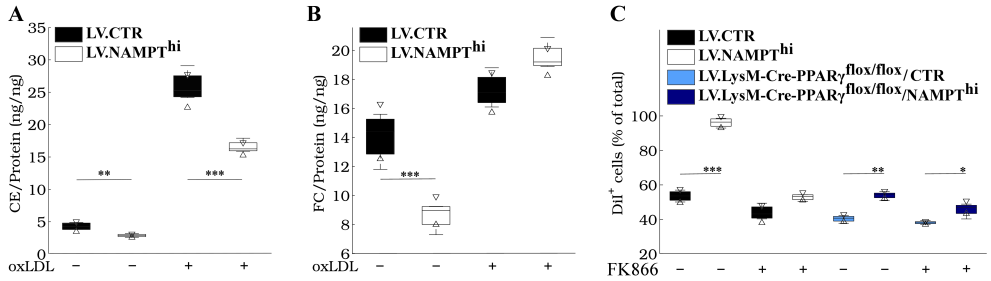

Figure. 3.7. *iNAMPT modulate lipid homeostasis in macrophages via PPARγ. A-B. Cholesterol ester (A) and free cholesterol (B) accumulation in BMDM over expressing iNAMPT, after 24 h incubation with oxLDL (50μg protein/ml). C. Quantification of DiI–oxLDL uptake by PPARγ deficient BMDM infected with LV.CTR (sky blue) or LV.NAMPT^{hi} (dark blue) lentivirus. DiI$^+$ cells were quantified after 24 h incubation with FK866 (500 nM). Data as mean ±SEM. $*P \leq 0.05$, $**P \leq 0.01$, $***P \leq 0.001$, n =4.*

iNAMPT and PPARγ Expression Are Tightly Correlated in Human Atherosclerosis To verify whether the disclosed mutual interaction between iNAMPT and PPARγ is also relevant in the context of human disease, PPARγ expression levels were assessed in atherosclerotic and non–atherosclerotic vessels obtained from carotid lesion and common iliac artery of organ donors, respectively, and in a carotid artery cohort con-

taining early, advanced, and ruptured carotid plaque segments. The results of this analysis revealed a tight correlation between NAMPT and PPARγ expression in atherosclerotic (Appendix B. Fig. B5A) but not healthy arteries (Appendix B. Fig. B5B). In addition, a strong relationship between NAMPT and PPARγ expression changes with progressive atherosclerotic disease was observed (Appendix B. Fig. B5C).

3.5 Discussion

In this study the role of iNAMPT in the genesis and development of atherosclerosis was addressed. Using a gain of function approach, the over expression of iNAMPT was demonstrated to confer protection against atherosclerosis by various mechanisms: first, by attenuating monocyte intravasation and migration in response to chemotactic signals; second, by reducing apoptosis of macrophages in response to oxLDL; third, skewing monocyte and macrophage differentiation into an anti–inflammatory M2 phenotype, and fourth; inducing over expression of genes involved in cholesterol efflux and attenuating lipid accumulation in macrophages. Taken together, the results indicate that iNAMPT participate in three hallmarks of atherosclerosis, i.e., leukocyte homeostasis, inflammation and lipid accumulation.

Overall, the effects imposed by over expressing of NAMPT, led to a significant decrease in plaque burden and delay in plaque progression in the aortic roots of LV.iNAMPT^{hi} chimeras, which however displayed equivalent plasma cholesterol and triglyceride levels, compared to control mice. In fact, lesions in iNAMPT^{hi} mice did not progress beyond a fatty streak stage, which was characterized by aortic lesions with low content of macrophages and marginal size of necrotic cores. The common pathway of apoptosis was minimally activated in aortic root lesions of iNAMPT^{hi} chimeras, indicating a protecting anti–apoptotic effect of NAMPT on lesion macrophages.

In agreement with these results, supra physiological iNAMPT levels, as induced by lentiviral gene transfer, caused increased levels of intracellular NAD$^+$ and resistance to apoptosis induction in macrophages upon exposure to oxLDL. In agreement with these findings, monocyte derived macrophages confronted with hypobaric hypoxia have been reported to display up–regulated expression of NAMPT [179].

Various molecular mechanism may be responsive for the protection from apoptosis observed upon NAMPT over expression: at the molecular level, NAMPT inhibits apoptosis by catalyzing the condensation of nicotinamide with 5–phosphoribosyl–1–pyrophosphate to yield nicotinamide mononucleotide, an intermediate in the biosynthesis of NAD$^+$; which in turn inhibits apoptosis through several mechanisms (Reviewed in [155]). over expression of NAMPT led to increased intracellular levels of NAD, likely causing increased intracellular NAD$^+$ dependent protection from apoptosis in atherosclerotic lesions of iNAMPT^{hi} chimeras.

Increased expression of SIRT1 and ATP binding cassette transporters (ABCA1 and ABCG1), as observed upon induction of NAMPT over expression, might have contributed to the resistance to apoptosis observed in macrophages of iNAMPT^{hi} chimeras, by increasing the deacetylation of p53 [183]; which has been demonstrated to promote survival through induction of autophagy [184,185] and induced reverse cholesterol transport thereby reducing the intracellular content of cytotoxic lipids, including free cholesterol [186]; and suppressing the oxidative burst mediated by NADPH oxi-

dase NOX_2, following exposure to oxidized phospholipids, which is known to induce programmed cell death [187]. In agreement with this, iNAMPT over expressing macrophages presented reduced accumulation of cholesterol esters and free cholesterol in vitro.

Reduced contents of macrophages were observed in atherosclerotic lesions of chimeric mice over expressing iNAMPT in hematopoietic cells. Mechanistically, iNAMPT over expression in macrophages causes PPARγ dependent downregulation of CCR2 and reduced extravasation, in agreement with the negative regulation that PPARγ has been reported to exert on CCR2 expression and chemotaxis [38, 188, 189] and the role of CCR2 in macrophage mobilization [190]. over expression of NAMPT also increased the expression of ATP binding cassette transporters ABCA1 and ABCG1 thereby reducing the intracellular accumulation of cholesterol esters and free cholesterol, in agreement with previously published data [191–195]. This effect of NAMPT over expression likely attenuated the formation of foam cell macrophages contributing to the delayed progression observed in atherosclerotic lesion of NAMPT over expressing chimeric mice.

Increased levels of myelocyte colony forming units were observed in bone marrow of iNAMPT^{hi} chimeras indicating increased myeloproliferation. In addition, absolute bone marrow monocyte counts were slightly increased upon NAMPT over expression. However circulating monocyte numbers were lower. Since iNAMPT^{hi} macrophages downregulated the expression of CCR2, which is critical for monocyte intravasation [190], these results suggest stromal sequestration causing reduced availability of circulatory monocytes to extravasate into atherosclerotic lesions in NAMPT over expressing chimeras. In agreement with this, administration of the NAMPT inhibitor FK866 [196], boosted resident bone marrow monocyte release and circulating monocyte numbers.

BMDM from iNAMPT^{hi} chimeras were hyporeactive to inducers of M1 differentiation and displayed stronger alternative activation in response to M2 stimulants by activation of PPARγ *in-vitro* and upregulation of PPARγ, SIRT1 ABCA1 and ABCG1, which likely induced lesion stabilization by modulation of macrophage differentiation [186,197–200]. PPARγ in particular inhibits the proinflammatory activation of macrophages in atherosclerosis [201,202], and positively regulates their alternative polarization [203,204].

In addition, hematopoietic NAMPT over expression caused a marked shift in circulatory monocyte subset balance characterized by lower CD11b^{+}Ly6c^{hi} and higher CD11b^{+}Ly6c^{lo} monocyte counts, which might have further reduced the M1/M2 macrophage ratio in atherosclerotic lesions as result of increased availability of Lyc6^{lo} monocytes to home into atherosclerotic lesions to differentiate into alternative activated macrophages (AAM) [205]. The upregulated expression of ABCA1 and ABCG1 upon NAMPT over expression observed might have also contributed to a higher Ly6c^{lo} to Ly6c^{hi} monocyte ratio, by negative regulation of hematopoietic stem cell progenitor extravasation and extramedullary hematopoiesis [206]; since hematopoietic stem cell progenitors constitute a source of CD11b^{+}Ly6c^{hi} monocytes in atherosclerosis upon extravasation out of the bone marrow and differentiation in the spleen [66].

Collectively, these results suggest that besides reduced macrophage accumulation due to impaired monocyte extravasation and stromal sequestration, iNAMPT^{hi} over expression might have caused skewed M2 macrophage differentiation in atheros-

clerotic lesions; likely contributing to the delayed progression and features of lesion stabilization observed, for M2 macrophages mediate wound healing and resolution of inflammation [207].

Surprisingly however, mRNA coding for NAMPT, displays a expression pattern characteristic of inflammatory monocytes [161, 162, 208] and CAM [179]. Besides, NAMPT is part of a cluster of human genes upregulated upon IFNγ and LPS stimulation and downregulated in response to IL–4 (Cluster C-IV, Fig. 2.9A-C, Page 36 in Chapter 2) whose expression is controlled by transcription factors linked to pro–inflammatory macrophage differentiation (Fig. 2.11, Page 38 in Chapter 2).

In addition, NAMPT and PPARγ were here demonstrated to be progressively upregulated in human atherosclerotic lesions and PBMCs obtained from patients with symptomatic carotid atherosclerosis. Furthermore, NAMPT expression is increased in unstable atherosclerotic carotid lesions, primarily in foam cell macrophages [162]. Similarly, NAMPT serum levels are significantly associated with higher intima–media thickness and advanced carotid atherosclerosis in patients with type 2 diabetes [209]; which suggest, contrary to our results, that NAMPT has pro–inflammatory and atherogenic functions.

Various reasons could be responsible for this paradox. First, the positive association between NAMPT and PPARγ upregulation in the context of human atherosclerotic lesion progression/vulnerability might be due to correlation without causation. In fact, studies using PPARγ activators in the clinical context have not provided conclusive evidence that they reduce cardiovascular morbidity and mortality, which may be related to adverse effects of PPARγ activation in human atherosclerosis [210]; despite activation of PPARγ has favorable effects on measures of adipocyte function, insulin sensitivity, lipoprotein metabolism, and vascular structure and function in experimental animals [201]. This suggest interspecies variation and indicates that further experimentation would be needed to investigate the relevance of the results here presented in the human context.

Another possibility is that PPARγ and NAMPT could be functional in gene networks that as a whole favor lesion progression and destabilization in advanced human atherosclerosis, despite they both participate in gene networks with anti–atherogenic functions. The fact that NAMPT and PPARG interact with genes having both functions, being part of networks N-I, N-II, N-III and N-IV (See Fig. 2.12, Page 39) argues for this possibility. Genes can contribute their molecular activities in multiple or even antagonistic biological processes due to their ability to interact with other genes in networks that as a whole execute cell processes and display emergent properties beyond single molecular functions of their particular constituents.

In conclusion, here we demonstrated that over expression of NAMPT in hematopoietic cells confers protection against high fat diet induced atherosclerosis in LDLr deficient mice. NAMPT acts upstream of PPARγ to upregulate ABCA1/ABCG1, thereby increasing macrophage lipid efflux, reducing apoptosis and inhibiting foam cell formation, while impairing extravasation and mobilization of monocytes out of the bone marrow and emulating PPARγ, SIRT1 and ABCA1/ABCG1 anti–inflammatory functions. These effects translated into delayed atherosclerotic lesion progression, reduced macrophage accumulation and features of lesion stability in atherosclerotic mice over expressing iNAMPThi, which contrasted to increased expression of NAMPT and PPARγ in human atherosclerosis.